

The real singlet scalar dark matter model

Wan-Lei Guo* and Yue-Liang Wu†

Kavli Institute for Theoretical Physics China,

Key Laboratory of Frontiers in Theoretical Physics,

Institute of Theoretical Physics, Chinese Academy of Science, Beijing 100190, China

Abstract

We present an undated comprehensive analysis for the simplest dark matter model in which a real singlet scalar with a Z_2 symmetry is introduced to extend the standard model. According to the observed dark matter abundance, we predict the dark matter direct and indirect detection cross sections for the whole parameter space. The Breit-Wigner resonance effect has been considered to calculate the thermally averaged annihilation cross section. It is found that three regions can be excluded by the current direct and indirect dark matter search experiments. In addition, we also discuss the implication of this model for the Higgs searches at colliders.

PACS numbers: 95.35.+d, 12.60.-i, 98.70.Sa

arXiv:1006.2518v3 [hep-ph] 16 Nov 2010

*Email: guowl@itp.ac.cn

†Email: ylwu@itp.ac.cn

I. INTRODUCTION

The existence of dark matter (DM) is by now well confirmed [1]. The recent cosmological observations have helped to establish the concordance cosmological model where the present Universe consists of about 73% dark energy, 23% dark matter, and 4% atoms [2]. Currently, several DM search experiments have found possible DM signals. The indirect DM detection experiments PAMELA [3], Fermi [4] and ATIC [5] have observed the cosmic electron anomalies which can be explained by annihilating or decaying DM models [6]. The direct DM detection experiment CDMS II [7] observed two possible events in the signal region. In addition, the DAMA/LIBRA [8] and CoGeNT [9] results favor a light DM candidate with a very large DM-nuclei elastic scattering cross section.

In the standard model (SM) of particle physics, there is no candidate for dark matter. Therefore, one has to extend the SM to account for the dark matter. It is well known that the simplest DM model can be constructed by adding a real singlet scalar S to the standard model. In this model, a discrete Z_2 symmetry ($S \rightarrow -S$) has to be introduced to make the DM candidate S stable. Although this model is very simple, it is phenomenologically interesting. Motivated by the simplicity and predictability, a number of authors have explored its phenomenology [10–16]. These research works are very helpful for us to understand some more complicated DM models.

In this paper, we try to give a comprehensive analysis for the real singlet scalar DM model. Instead of assuming the fixed Higgs mass, we scan the whole parameter space of the DM and Higgs masses. For the resonance case, one should consider the Breit-Wigner resonance effect. Once the coupling between DM particle and Higgs boson is derived from the observed DM abundance, the DM elastic scattering cross section on a nucleon and the DM annihilation cross section in the galactic halo can be straightly calculated. The current DM direct and indirect detection experiments can be used to constrain the model parameter space. In addition, we also discuss the Higgs searches at colliders when the Higgs can decay into two DM particles. This paper is organized as follows: In Sec. II, we outline the main features of this model and give the DM annihilation cross sections. In Sec. III, we investigate the DM direct search, the DM indirect search and the collider implications. Some discussions and conclusions are given in Sec. IV.

II. THE REAL SINGLET SCALAR DARK MATTER MODEL

In the real singlet scalar DM model, the Lagrangian reads

$$\mathcal{L} = \mathcal{L}_{\text{SM}} + \frac{1}{2} \partial_\mu S \partial^\mu S - \frac{m_0^2}{2} S^2 - \frac{\lambda_S}{4} S^4 - \lambda S^2 H^\dagger H, \quad (1)$$

where H is the SM Higgs doublet. The linear and cubic terms of the scalar S are forbidden by the Z_2 symmetry $S \rightarrow -S$. Then S has a vanishing vacuum expectation value (VEV) which ensures the DM candidate S stable. λ_S describes the DM self-interaction strength which is independent of the DM annihilation. The observations of galactic DM halos and the dynamics of the Bullet cluster may constrain λ_S when the DM mass is the order of 1 to 100 MeV [17]. Notice that the one-loop vacuum stability can lead to a lower bound on the DM mass for a given λ_S [15]. It is clear that the DM-Higgs coupling λ is the only one free parameter to control the DM annihilation. After the spontaneous symmetry breaking, one can obtain the DM mass $m_D^2 = m_0^2 + \lambda v_{\text{EW}}^2$ with $v_{\text{EW}} = 246$ GeV. It is natural for us to take m_D in the range of a few GeV and a few hundred GeV. In this paper, we focus on $10 \text{ GeV} \leq m_D \leq 200 \text{ GeV}$. In addition, the Higgs mass m_h is also an important parameter for our numerical calculation. The 95% confidence-level (CL) lower bound on the Higgs mass is $m_h > 114.4 \text{ GeV}$ given by the LEP accelerator [18]. The upper limit is $m_h < 186 \text{ GeV}$ when we consider the precision electroweak data and the LEP direct lower limit [19]. Therefore, we choose $114.4 \text{ GeV} < m_h < 186 \text{ GeV}$. It is worthwhile to stress that the current Tevatron experiments CDF and D0 have excluded $162 \text{ GeV} < m_h < 166 \text{ GeV}$ [20].

The real singlet scalar DM model is very simple and has only three free parameters m_D , m_h and λ . Based on the DM mass m_D , the DM candidate S may annihilate into fermion pairs, gauge boson pairs or Higgs pairs. The annihilation cross sections $\hat{\sigma} = 4E_1 E_2 \sigma v$ (E_1 and E_2 are the energies of two incoming DM particles) for different annihilation channels have the following forms:

$$\hat{\sigma}_{ff} = \sum_f \frac{\lambda^2 m_f^2}{\pi} \frac{1}{(s - m_h^2)^2 + m_h^2 \Gamma_h^2} \frac{(s - 4m_f^2)^{1.5}}{\sqrt{s}}, \quad (2)$$

$$\hat{\sigma}_{ZZ} = \frac{\lambda^2}{4\pi} \frac{s^2}{(s - m_h^2)^2 + m_h^2 \Gamma_h^2} \sqrt{1 - \frac{4m_Z^2}{s}} \left(1 - \frac{4m_Z^2}{s} + \frac{12m_Z^4}{s^2} \right), \quad (3)$$

$$\hat{\sigma}_{WW} = \frac{\lambda^2}{2\pi} \frac{s^2}{(s - m_h^2)^2 + m_h^2 \Gamma_h^2} \sqrt{1 - \frac{4m_W^2}{s}} \left(1 - \frac{4m_W^2}{s} + \frac{12m_W^4}{s^2} \right), \quad (4)$$

$$\hat{\sigma}_{hh} = \frac{\lambda^2}{4\pi} \sqrt{1 - \frac{4m_h^2}{s}} \left[\left(\frac{s + 2m_h^2}{s - m_h^2} \right)^2 - \frac{16\lambda v_{\text{EW}}^2}{s - 2m_h^2} \frac{s + 2m_h^2}{s - m_h^2} F(\xi) + \frac{32\lambda^2 v_{\text{EW}}^4}{(s - 2m_h^2)^2} \left(\frac{1}{1 - \xi^2} + F(\xi) \right) \right], \quad (5)$$

where s is the squared center-of-mass energy. The quantity F is defined as $F(\xi) \equiv \text{arctanh}(\xi)/\xi$ with $\xi \equiv \sqrt{(s - 4m_h^2)(s - 4m_D^2)}/(s - 2m_h^2)$. When the DM annihilation nears a resonance, we should know the Higgs decay width Γ_h which is given by

$$\begin{aligned} \Gamma_h = & \frac{\sum m_f^2 (m_h^2 - 4m_f^2)^{1.5}}{8\pi v_{\text{EW}}^2 m_h^2} + \frac{m_h^3}{32\pi v_{\text{EW}}^2} \sqrt{1 - \frac{4m_Z^2}{m_h^2}} \left(1 - \frac{4m_Z^2}{m_h^2} + \frac{12m_Z^4}{m_h^4}\right) \\ & + \frac{m_h^3}{16\pi v_{\text{EW}}^2} \sqrt{1 - \frac{4m_W^2}{m_h^2}} \left(1 - \frac{4m_W^2}{m_h^2} + \frac{12m_W^4}{m_h^4}\right) + \frac{\lambda^2 v_{\text{EW}}^2 \sqrt{m_h^2 - 4m_D^2}}{8\pi m_h^2}. \end{aligned} \quad (6)$$

Here we have included the decay mode $h \rightarrow SS$ if $m_h > 2m_D$.

III. DARK MATTER SEARCHES

A. Dark matter relic density

The thermal-average of the annihilation cross section times the relative velocity $\langle\sigma v\rangle$ is a key quantity in the determination of the DM cosmic relic abundance. We adopt the usual single-integral formula for $\langle\sigma v\rangle$ [21]:

$$\langle\sigma v\rangle = \frac{1}{n_{EQ}^2} \frac{m_D}{64\pi^4 x} \int_{4m_D^2}^{\infty} \hat{\sigma}(s) \sqrt{s} K_1\left(\frac{x\sqrt{s}}{m_D}\right) ds, \quad (7)$$

with

$$n_{EQ} = \frac{g_i}{2\pi^2} \frac{m_D^3}{x} K_2(x), \quad (8)$$

$$\hat{\sigma}(s) = \hat{\sigma} g_i^2 \sqrt{1 - \frac{4m_D^2}{s}}, \quad (9)$$

where $K_1(x)$ and $K_2(x)$ are the modified Bessel functions. $x \equiv m_D/T$ and $g_i = 1$ is the internal degrees of freedom for the scalar dark matter S . Using the annihilation cross section $\hat{\sigma}$ in Eqs. (2-5), one can numerically calculate the thermally averaged annihilation cross section $\langle\sigma v\rangle$ by use of the above formulas.

The evolution of the DM abundance is given by the following Boltzmann equation [22]:

$$\frac{dY}{dx} = -\frac{x \mathbf{s}(x)}{H} \langle\sigma v\rangle (Y^2 - Y_{EQ}^2), \quad (10)$$

where $Y \equiv n/s(x)$ denotes the dark matter number density. The entropy density $\mathbf{s}(x)$ and the Hubble parameter H evaluated at $x = 1$ are given by

$$\mathbf{s}(x) = \frac{2\pi^2 g_* m_D^3}{45 x^3}, \quad (11)$$

$$H = \sqrt{\frac{4\pi^3 g_*}{45} \frac{m_D^2}{M_{\text{PL}}}}, \quad (12)$$

where $M_{\text{PL}} \simeq 1.22 \times 10^{19}$ GeV is the Planck energy. g_* is the total number of effectively relativistic degrees of freedom. The numerical results of g_* have been presented in Ref. [23]. Here we take the QCD phase transition temperature to be 150 MeV.

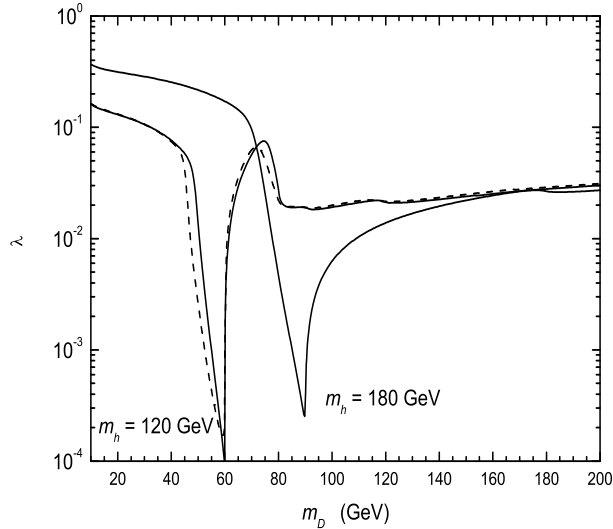


FIG. 1: The predicted coupling λ as a function of the DM mass m_D from the observed DM abundance for the $m_h = 120$ GeV and $m_h = 180$ GeV cases. The dashed line denotes the constant $\langle\sigma v\rangle$ case when its value is taken at the usual freeze-out temperature $x = 20$.

Using the result Y_0 of the integration of Eq. (10), we may obtain the DM relic density $\Omega_D h^2 = 2.74 \times 10^8 Y_0 m_D / \text{GeV}$. In terms of the observed DM abundance $0.1088 \leq \Omega_D h^2 \leq 0.1158$ [2], one can calculate the DM-Higgs coupling λ for the given m_D and m_h . As shown in Fig. 1, the observed DM abundance requires $\lambda \sim \mathcal{O}(10^{-4} - 10^{-1})$. It is well known that the annihilation cross section σ will become larger for the same coupling when the annihilation process nears a resonance. This feature implies that there is a very small coupling when $0.8 m_h \lesssim 2m_D < m_h$. This region is named as the resonance region in the following parts of this paper. It should be mentioned that the thermally averaged annihilation cross section $\langle\sigma v\rangle$ will significantly change as the evolution of the Universe when the DM particle is nearly one-half the mass of a resonance [24]. This is the Breit-Wigner resonance effect which has been used to explain the recent PAMELA, ATIC and Fermi anomalies. Here we have considered the Breit-Wigner resonance effect for the determination of the coupling λ . If we neglect the Breit-Wigner resonance effect and only consider the resonance

contribution, the predicted coupling λ will have distinct differences with the previous results. For illustration, we also present the corresponding λ in Fig. 1 by use of the constant $\langle\sigma v\rangle$ at $x = 20$. In this case, the predicted λ may differ from the correct one by more than a factor of 3 for the resonance region. Since the DM direct and indirect detection cross sections are proportional to λ^2 , one can derive the larger differences.

B. Dark matter direct search

For the scalar dark matter, the DM elastic scattering cross section on a nucleus \mathcal{N} is spin-independent, which is given by [1]

$$\sigma_{\mathcal{N}} = \frac{4M^2(\mathcal{N})}{\pi}(Zf_p + (A - Z)f_n)^2, \quad (13)$$

where $M(\mathcal{N}) = m_D M_{\mathcal{N}} / (m_D + M_{\mathcal{N}})$ and $M_{\mathcal{N}}$ is the target nucleus mass. Z and $A - Z$ are the numbers of protons and neutrons in the nucleus. $f_{p,n}$ is the coupling between DM and protons or neutrons, given by

$$f_{p,n} = \sum_{q=u,d,s} f_{Tq}^{(p,n)} a_q \frac{m_{p,n}}{m_q} + \frac{2}{27} f_{TG}^{(p,n)} \sum_{q=c,b,t} a_q \frac{m_{p,n}}{m_q}, \quad (14)$$

where $f_{Tu}^{(p)} = 0.020 \pm 0.004$, $f_{Td}^{(p)} = 0.026 \pm 0.005$, $f_{Ts}^{(p)} = 0.118 \pm 0.062$, $f_{Tu}^{(n)} = 0.014 \pm 0.003$, $f_{Td}^{(n)} = 0.036 \pm 0.008$ and $f_{Ts}^{(n)} = 0.118 \pm 0.062$ [25]. The coupling $f_{TG}^{(p,n)}$ between DM and gluons from heavy quark loops is obtained from $f_{TG}^{(p,n)} = 1 - \sum_{q=u,d,s} f_{Tq}^{(p,n)}$, which leads to $f_{TG}^{(p)} \approx 0.84$ and $f_{TG}^{(n)} \approx 0.83$. The results of DM-nucleus elastic scattering experiments are presented in the form of a normalized DM-nucleon scattering cross section σ_n^{SI} in the spin-independent case, which is straightforward

$$\sigma_n^{SI} = \left(\frac{m_D m_n}{m_D + m_n} \right)^2 \frac{1}{A^2 M^2(\mathcal{N})} \sigma_{\mathcal{N}} \approx \frac{4}{\pi} \left(\frac{m_D m_n}{m_D + m_n} \right)^2 f_n^2, \quad (15)$$

where we have used $f_p \approx f_n$.

In the real singlet scalar DM model, the DM candidate S interacts with nucleus \mathcal{N} through t -channel Higgs exchange. In this case, the DM-quark coupling a_q in Eq. (14) is given by

$$a_q = \frac{\lambda m_q}{m_D m_h^2}. \quad (16)$$

Using the predicted λ from the observed DM abundance, one can calculate the spin-independent DM-nucleon elastic scattering cross section σ_n^{SI} for the given m_D and m_h . We perform a numerical

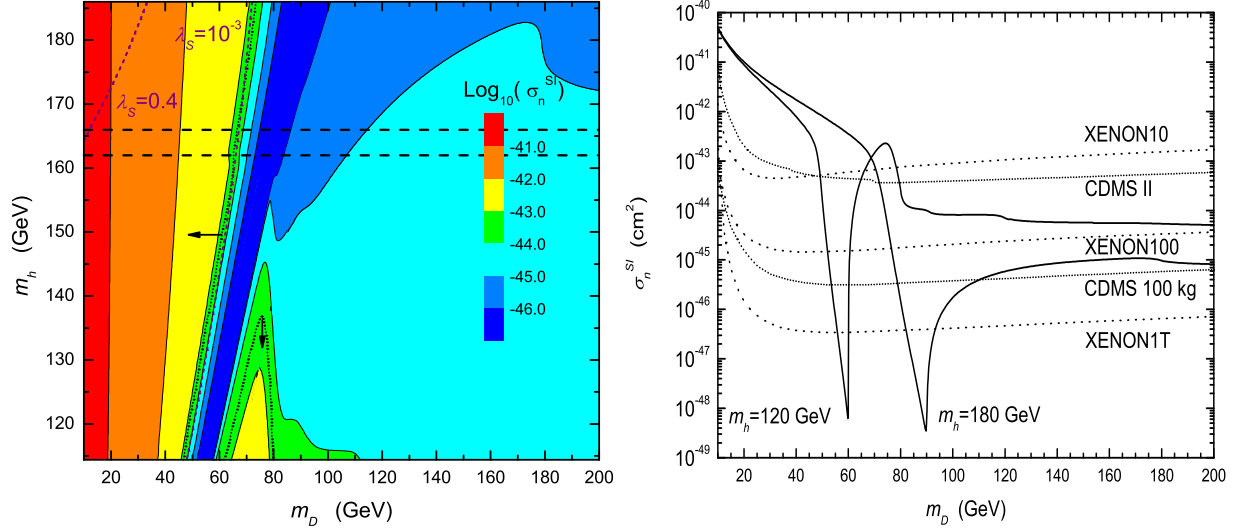


FIG. 2: The predicted DM-nucleon scattering cross section σ_n^{SI} for the whole parameter space. The short dotted lines with arrowhead indicate the excluded regions from the DM direct search experiments CDMS II and XENON10. The region among two dashed lines ($162 \text{ GeV} < m_h < 166 \text{ GeV}$) can be excluded by the Tevatron experiments CDF and D0. Two purple short dashed lines describe the minimum m_D allowed by both the DM observed abundance and the vacuum stability/perturbativity for $\lambda_S = 10^{-3}$ and $\lambda_S = 0.4$. The right panel corresponds to two fixed Higgs mass cases with current and future experimental upper bounds.

scan over the whole parameter space of m_D and m_h . The numerical results are shown in Fig. 2. For illustration, we have also plotted σ_n^{SI} as a function of m_D for the $m_h = 120 \text{ GeV}$ and $m_h = 180 \text{ GeV}$ cases. In view of the current DM direct detection upper bounds from CDMS II [7] and XENON10 [26], we find that two regions indicated by short dotted lines can be excluded. The future experiments XENON100 [27], CDMS 100 kg [28] and XENON1T [29] can cover most parts of the allowed parameter space. For the resonance region, the predicted σ_n^{SI} is far below the current experimental upper bounds. In Fig. 2, we also plot the minimum m_D allowed by both the DM observed abundance and the vacuum stability/perturbativity for the DM self-coupling $\lambda_S = 10^{-3}$ and $\lambda_S = 0.4$ when the cutoff scale is taken to be 1 TeV [15]. Increasing the cutoff scale, one can derive much stronger bounds [15]. In addition, the region among two dashed lines ($162 \text{ GeV} < m_h < 166 \text{ GeV}$) can be excluded by the Tevatron experiments CDF and D0.

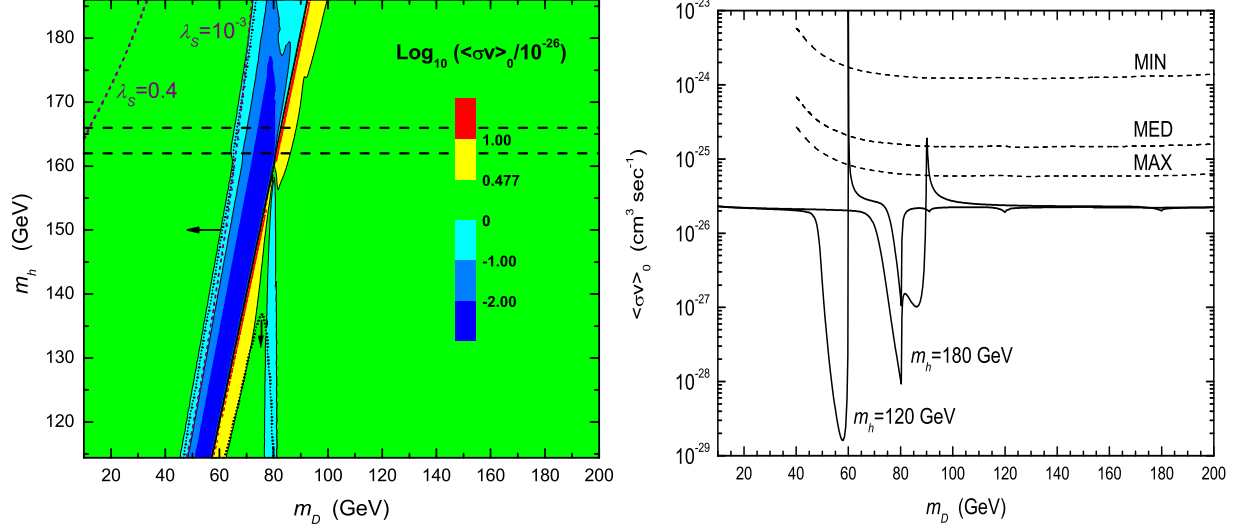


FIG. 3: The predicted thermally averaged DM annihilation cross section $\langle\sigma v\rangle_0$. The right panel corresponds to two fixed Higgs mass cases.

C. Dark matter indirect search

The DM indirect search experiments are designed to detect the DM annihilation productions which include neutrinos, gamma rays, electrons, positrons, protons and antiprotons. Since these methods are complementary to the direct detection, it will be very important for us to investigate the DM indirect detection. In order to derive the correct relic density, we have calculated the thermally averaged annihilation cross section $\langle\sigma v\rangle$ which depends on the temperature of the Universe. On the other hand, $\langle\sigma v\rangle$ also determines the DM annihilation rate in the galactic halo. The only difference among the above two cases is the temperature T . For the relic density, $\langle\sigma v\rangle$ is usually evaluated at the freeze-out temperature $x \approx 20$ (the averaged velocity $v \approx \sqrt{3/x}$). The dark matter annihilation in the galactic halo occurs at $x \approx 3 \times 10^6$ ($v \approx 10^{-3}$). Therefore we should calculate the thermally averaged annihilation cross section at $x \approx 3 \times 10^6$, namely $\langle\sigma v\rangle_0$. The numerical results have been shown in Fig. 3. One may find $1 \times 10^{-26} \text{ cm}^3 \text{ sec}^{-1} \leq \langle\sigma v\rangle_0 \leq 3 \times 10^{-26} \text{ cm}^3 \text{ sec}^{-1}$ for most parts of the parameter space, which is consistent with the usual s -wave annihilation cross section $\langle\sigma v\rangle \approx 3 \times 10^{-26} \text{ cm}^3 \text{ sec}^{-1}$ at the freeze-out temperature $x \approx 20$. However, the Breit-Wigner resonance effect can enhance or suppress $\langle\sigma v\rangle$ for the resonance case [24]. As shown in Fig. 3, $\langle\sigma v\rangle$ in the red and yellow regions is enhanced by the Breit-Wigner enhancement mechanism. Contrarily, $\langle\sigma v\rangle$ is suppressed ($\langle\sigma v\rangle \ll 1 \times 10^{-26} \text{ cm}^3 \text{ sec}^{-1}$) when double DM mass $2m_D$ is slightly

less than the Higgs mass m_h . In this case, it is very difficult for us to detect the signals of the DM annihilation. The vertical cyan region around 80 GeV has smaller $\langle\sigma v\rangle_0$ which originates from the threshold effect [30]. If m_D is slightly less than the W boson mass, the channel $SS \rightarrow W^+W^-$ is open at high temperature. It dominates the total thermally averaged annihilation cross section and determines the DM relic density. However, this channel is forbidden in the galactic halo (low relative velocity). At this moment, the channel $SS \rightarrow b\bar{b}$ has the dominant contribution. This feature can be well understood from Fig. 3 (right panel).

In our model, the DM annihilation can generate primary antiprotons which can be detected by the DM indirect search experiments. Recently, the PAMELA collaboration reports that the observed antiproton data is consistent with the usual estimation value of the secondary antiproton [3]. Therefore one can use the PAMELA antiproton measurements to constrain $\langle\sigma v\rangle_0$. In Fig. 3, we have also plotted the maximum allowed $\langle\sigma v\rangle_0$ for the MIN, MED and MAX antiproton propagation models [14]. Notice that a fixed Higgs mass $m_h = 120$ GeV has been assumed in Ref. [14]. The above upper bounds are still valid for our analysis when $m_D < 114.4$ GeV. Then we can find that a very narrow region can be excluded by the PAMELA antiproton data in our model. This feature is not shown in Ref. [14]. In fact, the width of this excluded region is about 0.4 GeV if we require $\langle\sigma v\rangle_0 \lesssim 10^{-25} \text{ cm}^3 \text{ sec}^{-1}$. For the MED and MAX propagation cases, the sensitivity of the future experiment AMS-02 [31] may reach $\langle\sigma v\rangle_0 \sim \mathcal{O}(10^{-27} - 10^{-26}) \text{ cm}^3 \text{ sec}^{-1}$ [14], which can cover most parts of the whole parameter space as shown in Fig. 3.

D. Implications on the Higgs search

Since the DM candidate S has substantial coupling to nucleons via Higgs boson exchange, they can be produced in high energy collider experiments such as the Tevatron and Large Hadron Collider (LHC). If $m_h > 2m_D$, the decay channel $h \rightarrow 2S$ is kinematically allowed. In this case, two DM particle production may be associated with the Higgs production. The produced DM particles are invisible and have the missing energy signals. This will affect the usual SM Higgs searches at the Tevatron and LHC. To describe this effect, we calculate the branching ratio of the Higgs visible decay [11]

$$\text{BR}_{\text{visible}} = \frac{\Gamma_{h \rightarrow \text{SM}}}{\Gamma_{h \rightarrow 2S} + \Gamma_{h \rightarrow \text{SM}}} . \quad (17)$$

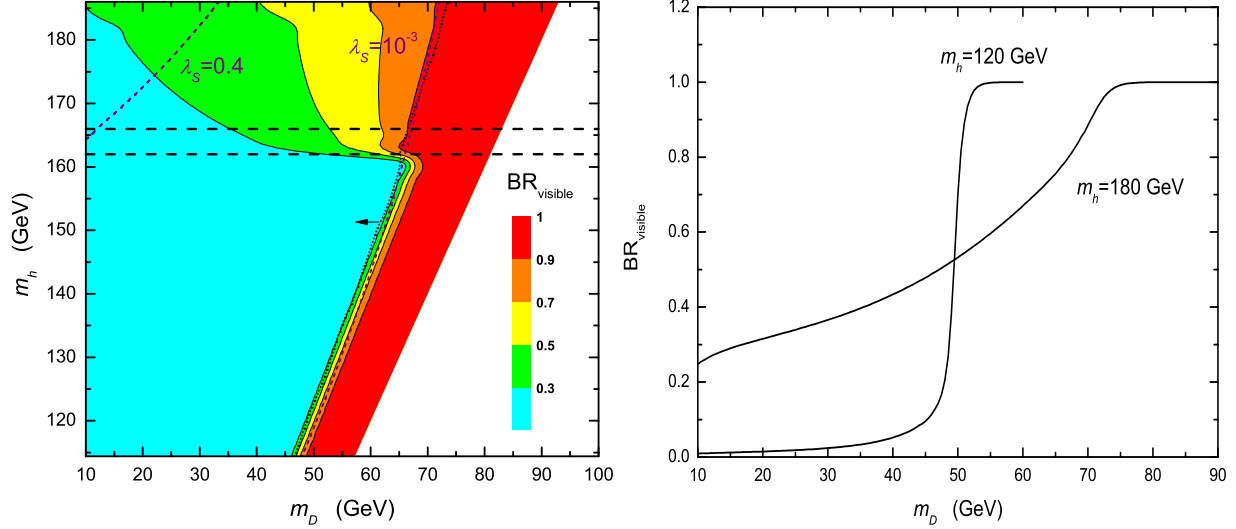


FIG. 4: The predicted branching ratio of the Higgs visible decay BR_{visible} . The right panel corresponds to two fixed Higgs mass cases.

The numerical results have been shown in Fig. 4. Considering the constraints from the DM direct search experiments, we find $BR_{\text{visible}} \gtrsim 0.3$. In fact, we have $BR_{\text{visible}} > 0.9$ for most parts of the allowed parameter space. If the future CDMS 100 kg does not observe the DM signals, the region less than 0.9 can be excluded. Notice that the invisible Higgs decays in the allowed region $0.3 \lesssim BR_{\text{visible}} \lesssim 0.75$ can be identified at the ATLAS with an integrated luminosity of 30 fb^{-1} [32]. The decay mode $h \rightarrow SS$ can lower the statistical significance of the traditional Higgs search at the CMS [13]. A combined analysis of the traditional visible search and the invisible search at the LHC can enhance the discovery reach and the possibility of distinguishing this DM model from the SM [13].

IV. DISCUSSION AND CONCLUSION

We have detailedly discussed the $10 \text{ GeV} \leq m_D \leq 200 \text{ GeV}$ case. As shown in Fig. 2, one can obtain the very large DM-nucleon elastic scattering cross section $\sigma_n^{SI} \sim \mathcal{O}(10^{-41} \text{ cm}^2)$ for $m_D \sim 10 \text{ GeV}$. In this case, the light DM particle S can explain the DAMA/LIBRA and CoGeNT experiments [16]. It should be mentioned that this explanation is consistent with the XENON10 and CDMS null results [33]. Currently, the XENON100 preliminary results challenge the DM interpretation of the DAMA/LIBRA and CoGeNT signals [34]. However, there are bifurcations

on the choice of the ratio between electron equivalent energy and nuclear recoil energy [35]. If $m_D > 200$ GeV, one will not meet the resonance and the new annihilation channels. Then $\langle\sigma v\rangle_0 \approx 2.3 \times 10^{-26} \text{ cm}^3 \text{ sec}^{-1}$ and $10^{-45} \text{ cm}^2 \lesssim \sigma_n^{SI} \lesssim 10^{-44} \text{ cm}^2$ can be derived.

In conclusion, we have made an undated comprehensive analysis for the whole parameter space of the real singlet scalar DM model. To satisfy the observed DM abundance, we numerically solve the Boltzmann equation and predict the DM-Higgs coupling λ which determines the DM direct and indirect detection rates. We demonstrate that the Breit-Wigner resonance effect can significantly change the predicted coupling λ by more than a factor of 3 for the resonance region. The spin-independent DM-nucleon elastic scattering cross section σ_n^{SI} has been presented for the whole parameter space of m_D and m_h . One may find that the current experimental upper bounds from CDMS II and XENON10 can exclude two regions. For the DM indirect detection, we calculate the thermally averaged annihilation cross section $\langle\sigma v\rangle_0$ which can be enhanced or suppressed by the Breit-Wigner resonance effect. We find that a very narrow region can be excluded by the PAMELA antiproton measurements. One should notice that the predicted σ_n^{SI} and $\langle\sigma v\rangle_0$ are very small for the resonance region. In this case, it is very difficult for us to detect the signals of the DM annihilation. However, we still have possibility to test the resonance region as detector masses of DM direct search experiments become larger. When the decay channel $h \rightarrow SS$ is kinematically allowed, we find that the allowed branching ratio of the Higgs visible decay satisfy $\text{BR}_{\text{visible}} \gtrsim 0.3$. If the future CDMS 100 kg does not observe the DM signals, the region less than 0.9 can be excluded.

Acknowledgments

This work is supported in part by the National Basic Research Program of China (973 Program) under Grants No. 2010CB833000; the National Nature Science Foundation of China (NSFC) under Grants No. 10821504 and No. 10905084; and the Project of Knowledge Innovation Program (PKIP) of the Chinese Academy of Science.

-
- [1] For reviews, see, e.g., G. Jungman, M. Kamionkowski and K. Griest, Phys. Rept. **267**, 195 (1996); G. Bertone, D. Hooper and J. Silk, Phys. Rept. **405**, 279 (2005).
 [2] E. Komatsu *et al.*, arXiv:1001.4538 [astro-ph.CO].

- [3] O. Adriani *et al.* [PAMELA Collaboration], *Nature* **458**, 607 (2009) [arXiv:0810.4995 [astro-ph]]; *Phys. Rev. Lett.* **102**, 051101 (2009) [arXiv:0810.4994 [astro-ph]].
- [4] A. A. Abdo *et al.* [The Fermi LAT Collaboration], *Phys. Rev. Lett.* **102**, 181101 (2009) [arXiv:0905.0025 [astro-ph.HE]].
- [5] J. Chang *et al.*, *Nature* **456**, 362 (2008).
- [6] W. L. Guo, Y. L. Wu and Y. F. Zhou, *Phys. Rev. D* **81**, 075014 (2010) [arXiv:1001.0307 [hep-ph]]; and references therein.
- [7] Z. Ahmed *et al.* [The CDMS-II Collaboration], arXiv:0912.3592 [astro-ph.CO].
- [8] R. Bernabei *et al.* [DAMA Collaboration], *Eur. Phys. J. C* **56**, 333 (2008) [arXiv:0804.2741 [astro-ph]].
- [9] C. E. Aalseth *et al.* [CoGeNT collaboration], arXiv:1002.4703 [astro-ph.CO].
- [10] J. McDonald, *Phys. Rev. D* **50**, 3637 (1994) [arXiv:hep-ph/0702143].
- [11] C. P. Burgess, M. Pospelov and T. ter Veldhuis, *Nucl. Phys. B* **619**, 709 (2001) [arXiv:hep-ph/0011335].
- [12] M. C. Bento, O. Bertolami, R. Rosenfeld and L. Teodoro, *Phys. Rev. D* **62**, 041302 (2000) [arXiv:astro-ph/0003350]; C. Bird, P. Jackson, R. V. Kowalewski and M. Pospelov, *Phys. Rev. Lett.* **93**, 201803 (2004) [arXiv:hep-ph/0401195]; H. Davoudiasl, R. Kitano, T. Li and H. Murayama, *Phys. Lett. B* **609**, 117 (2005) [arXiv:hep-ph/0405097]; G. Cynolter, E. Lendvai and G. Pocsik, *Acta Phys. Polon. B* **36**, 827 (2005) [arXiv:hep-ph/0410102]; S. h. Zhu, arXiv:hep-ph/0601224; X. G. He, T. Li, X. Q. Li and H. C. Tsai, *Mod. Phys. Lett. A* **22**, 2121 (2007) [arXiv:hep-ph/0701156]; S. Andreas, T. Hambye and M. H. G. Tytgat, *JCAP* **0810**, 034 (2008) [arXiv:0808.0255 [hep-ph]]; C. E. Yaguna, *JCAP* **0903**, 003 (2009) [arXiv:0810.4267 [hep-ph]]; X. G. He, T. Li, X. Q. Li, J. Tandean and H. C. Tsai, *Phys. Rev. D* **79**, 023521 (2009) [arXiv:0811.0658 [hep-ph]]; W. L. Guo, L. M. Wang, Y. L. Wu, Y. F. Zhou and C. Zhuang, *Phys. Rev. D* **79**, 055015 (2009) [arXiv:0811.2556 [hep-ph]]; B. Grzadkowski and J. Wudka, *Phys. Rev. Lett.* **103**, 091802 (2009) [arXiv:0902.0628 [hep-ph]]; K. Kohri, J. McDonald and N. Sahu, *Phys. Rev. D* **81**, 023530 (2010) [arXiv:0905.1312 [hep-ph]]; X. G. He, T. Li, X. Q. Li, J. Tandean and H. C. Tsai, *Phys. Lett. B* **688**, 332 (2010) [arXiv:0912.4722 [hep-ph]]; M. Farina, D. Pappadopulo and A. Strumia, *Phys. Lett. B* **688**, 329 (2010) [arXiv:0912.5038 [hep-ph]]; X. G. He, S. Y. Ho, J. Tandean and H. C. Tsai, arXiv:1004.3464 [hep-ph]; C. Arina, F. X. Josse-Michaux and N. Sahu, arXiv:1004.3953 [hep-ph]; S. Kanemura, S. Matsumoto, T. Nabeshima and N. Okada, arXiv:1005.5651 [hep-ph].

- [13] V. Barger, P. Langacker, M. McCaskey, M. J. Ramsey-Musolf and G. Shaughnessy, Phys. Rev. D **77**, 035005 (2008) [arXiv:0706.4311 [hep-ph]]; Phys. Rev. D **79**, 015018 (2009) [arXiv:0811.0393 [hep-ph]].
- [14] A. Goudelis, Y. Mambrini and C. Yaguna, JCAP **0912**, 008 (2009) [arXiv:0909.2799 [hep-ph]].
- [15] M. Gonderinger, Y. Li, H. Patel and M. J. Ramsey-Musolf, JHEP **1001**, 053 (2010) [arXiv:0910.3167 [hep-ph]].
- [16] A. Bandyopadhyay, S. Chakraborty, A. Ghosal and D. Majumdar, arXiv:1003.0809 [hep-ph]; S. Andreas, C. Arina, T. Hambye, F. S. Ling and M. H. G. Tytgat, arXiv:1003.2595 [hep-ph].
- [17] J. McDonald, N. Sahu and U. Sarkar, JCAP **0804**, 037 (2008) [arXiv:0711.4820 [hep-ph]].
- [18] R. Barate *et al.* [LEP Working Group for Higgs boson searches and ALEPH Collaboration and and], Phys. Lett. B **565**, 61 (2003) [arXiv:hep-ex/0306033].
- [19] J. Alcaraz [ALEPH Collaboration and CDF Collaboration and D0 Collaboration and an], arXiv:0911.2604 [hep-ex].
- [20] T. Aaltonen *et al.* [CDF and D0 Collaborations], Phys. Rev. Lett. **104**, 061802 (2010) [arXiv:1001.4162 [hep-ex]].
- [21] J. Edsjo and P. Gondolo, Phys. Rev. D **56**, 1879 (1997) [arXiv:hep-ph/9704361].
- [22] E. W. Kolb and M. S. Turner, *The Early Universe* (Addison-Wesley, Reading, MA, 1990).
- [23] P. Gondolo and G. Gelmini, Nucl. Phys. **B360**, 145 (1991).
- [24] D. Feldman, Z. Liu and P. Nath, Phys. Rev. D **79**, 063509 (2009) [arXiv:0810.5762 [hep-ph]]; M. Ibe, H. Murayama and T. T. Yanagida, Phys. Rev. D **79**, 095009 (2009) [arXiv:0812.0072 [hep-ph]]; W. L. Guo and Y. L. Wu, Phys. Rev. D **79**, 055012 (2009) [arXiv:0901.1450 [hep-ph]].
- [25] J. R. Ellis, A. Ferstl and K. A. Olive, Phys. Lett. B **481**, 304 (2000) [arXiv:hep-ph/0001005].
- [26] J. Angle *et al.* [XENON Collaboration], Phys. Rev. Lett. **100**, 021303 (2008) [arXiv:0706.0039 [astro-ph]].
- [27] E. Aprile [Xenon Collaboration], J. Phys. Conf. Ser. **203**, 012005 (2010).
- [28] J. Cooley, SLAC seminar on Dec. 17, 2009; L. Hsu, Fermilab seminar on Dec. 17, 2009.
- [29] Elena Aprile, XENON1T: a ton scale Dark Matter Experiment , presented at UCLA Dark Matter 2010, February 26, 2010. The XENON1000 project in China has been supported in part by the National Basic Research Program of China (973 Program).
- [30] K. Griest and D. Seckel, Phys. Rev. D **43**, 3191 (1991).
- [31] <http://ams.cern.ch/>

- [32] M. Warsinsky [ATLAS Collaboration], *J. Phys. Conf. Ser.* **110**, 072046 (2008).
- [33] F. Petriello and K. M. Zurek, *JHEP* **0809**, 047 (2008) [arXiv:0806.3989 [hep-ph]]; C. Savage, G. Gelmini, P. Gondolo and K. Freese, *JCAP* **0904**, 010 (2009) [arXiv:0808.3607 [astro-ph]].
- [34] E. Aprile *et al.* [XENON100 Collaboration], arXiv:1005.0380 [astro-ph.CO].
- [35] J. I. Collar and D. N. McKinsey, arXiv:1005.0838 [astro-ph.CO].